RMetS
Royal Meteorological Society

The effect of urbanisation on the climatology of thunderstorm initiation

Alex M. Haberlie,[a,b]* Walker S. Ashley[a,b] and Thomas J. Pingel[b]
[a]*Meteorology Program, Northern Illinois University, De Kalb, USA*
[b]*Department of Geography, Northern Illinois University, De Kalb, USA*

*Correspondence to: A. M. Haberlie, Department of Geography, Northern Illinois University, De Kalb, IL 60115, USA.
E-mail: ahaberlie@niu.edu

This study assesses the impact of urban land use on the climatological distribution of thunderstorm initiation occurrences in the humid subtropical region of the southeast United States, which includes the Atlanta, Georgia metropolitan area. Initially, an automated technique is developed to extract the locations of isolated convective initiation (ICI) events from 17 years (1997–2013) of composite reflectivity radar data for the study area. Nearly 26 000 ICI points were detected during 85 warm-season months, providing the foundation for first long-term, systematic assessment of the influence of urban land use on thunderstorm development. Results reveal that ICI events occur more often over the urban area compared to its surrounding rural counterparts, confirming that anthropogenic-induced changes in land cover in moist tropical environments lead to more initiation events, resulting thunderstorms and affiliated hazards over the developed area. The ICI risk for Atlanta is greatest during the late afternoon and early evening in July and August in synoptically benign conditions. Greater ICI counts downwind of Atlanta suggest that prevailing wind direction also influences the location of these events. Moreover, ICI occurrences over the city were significantly higher on weekdays compared to weekend days – a result that was not apparent in a rural control region located west of the city. This suggests that the weekly commuting cycle and associated aerosol levels of Atlanta may amplify ICI rates. The investigation provides a methodological framework for future studies that examine the effect of land use, land cover, and terrain discontinuities on the spatio-temporal character of ICI events.

Key Words: urban climatology; convective initiation; image analysis; anthropogenic climate change

Received 17 September 2014; Revised 20 November 2014; Accepted 24 November 2014; Published online in Wiley Online Library

1. Introduction

As urban, suburban and exurban growth continues in the United States (Nowak and Walton, 2005; Theobald, 2005), it will become increasingly likely that weather hazards will impact human interests due to the so-called 'expanding bull's eye effect' (Ashley *et al*, 2014). Compounding this issue, the atmospheric effects caused by developed land use include an increased probability of thunderstorm activity over and around a city (e.g. Dixon and Mote, 2003; Shepherd, 2005; Mote *et al*, 2007; Bentley *et al*, 2010; Paulikas and Ashley, 2011; Ashley *et al*, 2012; Coquillat *et al*, 2012; Ganeshan *et al*, 2013; Stallins *et al*, 2013). The combination of these factors results in areas of enhanced exposure in urban areas to thunderstorm hazards.

To quantify potential regions of enhanced exposure and to assess how urban landscapes modify thunderstorm formation, we pose the question: '*Do areas near Atlanta experience more isolated convective initiation (ICI) events than rural counterparts?*' This is an important question to address because a regional understanding of ICI occurrence distribution could alert residents of particular locations in and around an urban area of elevated risk to life and property (Stallins, 2002; Stewart *et al*, 2004; Shepherd *et al*, 2011). Further, because a developing thunderstorm may produce hazardous weather with little to no lead time, discovering the spatial patterns of increased ICI activity could lead to greater awareness for local forecasters and the general public. Uncovering these spatial patterns would also advance our understanding of the climatological impacts caused by land use/land cover change associated with urban areas – a research direction that has been labelled as integral to understanding anthropogenic climate change (Shepherd, 2005; Mahmood *et al*, 2010, 2014; Georgescu *et al*, 2014). Our study utilizes an automated technique to extract the locations of ICI events from radar images over the course of 85 warm-season months. We focus on Atlanta for this study because previous work has reported augmentation of convective activity over and around the city and it is in a region that experiences few instances of synoptic-scale forcing for ascent during the warm season (Ashley *et al*, 2012). This approach allows us to perform

a geostatistical analysis using an unprecedented sample size of ICI events, while also creating an experimental framework that permits a comparison of ICI activity around Atlanta to a rural control region (Lowry, 1998; Ashley *et al*, 2012). Here, we present the first objective, long-term climatology of land-use induced ICI events for Atlanta and the surrounding region.

2. Background

Studies such as METROMEX (Huff and Changnon, 1973) and more contemporary undertakings (e.g. Shepherd *et al*, 2002; Shepherd and Burian, 2003; Burian and Shepherd, 2005; Mote *et al*, 2007; Hand and Shepherd, 2009; Niyogi *et al*, 2011; Ashley *et al*, 2012; Ganeshan *et al*, 2013) have found evidence that urban areas modify regional precipitation climatology and produce climatological precipitation maxima within and downwind of the city. These maxima are thought to be the result of a combination of factors related to the diurnal impact of developed land on the atmosphere. Specifically, localized areas of enhanced instability and convergence induced by the urban heat island (UHI) and increased surface roughness associated with heavily developed land promote atmospheric conditions more favourable for precipitation development (Oke, 1973; Baik *et al*, 2001; Shepherd, 2005). These effects are similar to those induced by natural land-cover discontinuities such as soil moisture and vegetation boundaries (Taylor *et al*, 2007, 2010; Garcia-Carreras *et al*, 2010; Garcia-Carreras and Parker, 2011). The location of these enhanced rainfall swaths relative to urban areas have been linked to the prevailing wind direction in the mid-levels of the atmosphere (Rose *et al*, 2008; Hand and Shepherd, 2009; Ganeshan *et al*, 2013). Further, synoptically benign days (Mote *et al*, 2007) and days with conditional instability (Bentley *et al*, 2012) maximize the likelihood of urban effects on precipitation (Kalkstein *et al*, 1996; Sheridan *et al*, 2000; Sheridan, 2002; Mote *et al*, 2007; Ashley *et al*, 2012; Bentley *et al*, 2012). Urban aerosols are also thought to enhance urban-induced precipitation (Bell *et al*, 2008; Lacke *et al*, 2009; Coquillat *et al*, 2012; Stallins *et al*, 2013), but there is evidence that they may suppress rainfall amounts (Rosenfeld, 2000; Kaufmann *et al*, 2007; Koren *et al*, 2008; Diem, 2013) or produce mixed effects such as contributing to greater longevity of a precipitating cloud while having no effect on its initiation (van den Heever and Cotton, 2007).

Although many urban precipitation studies have used rain-gauge data (Blumenfeld, 2008; Hand and Shepherd, 2009), remotely sensed, quality-controlled products may be a better tool to characterize the short- to long-term effects of developed areas on regional hydroclimatology (Dixon and Mote, 2003; Ashley *et al*, 2012; Bentley *et al*, 2012). Recent studies on urban rainfall anomalies have used satellite precipitation estimates (Rosenfeld, 2000; Shepherd *et al*, 2002; Hand and Shepherd, 2009), lightning data (Bentley and Stallins, 2005; Stallins *et al*, 2005; Altaratz *et al*, 2010; Gauthier *et al*, 2010; Lang and Rutledge, 2011; Coquillat *et al*, 2012), and ground-based radar data (Dixon and Mote, 2003; Mote *et al*, 2007; Ashley *et al*, 2012; Bentley *et al*, 2012; Ganeshan *et al*, 2013). These studies have emphasized that thunderstorm activity should be more sensitive to urban effects and, as a result, some focus has shifted to creating thunderstorm occurrence climatologies instead of rain-gauge climatologies (Bentley and Stallins, 2005; Stallins *et al*, 2005; Ashley *et al*, 2012; Bentley *et al*, 2012). Radar data are ideal for these types of analyses as they have fine temporal and spatial resolution, are widely available, have a long and nearly continuous period of record, and allow opportunities for specific analyses that cannot be performed using other platforms (Parker and Knievel, 2005; Matyas, 2010).

Whereas lightning and thunderstorm occurrence climatologies have received much attention in the literature, convective initiation occurrence climatologies have not. This may be because researchers have more confidence in manual rather than automated approaches, which makes comprehensive, long-term, convective initiation climatologies unfeasible (Lakshmanan *et al*, 2009). Despite this, a wide variety of storm identification tracking algorithms exist and are used for climatological applications. These methods include SCIT (Johnson *et al*, 1998), TREC (Rinehart and Garvey, 1978), TITAN (Dixon and Wiener, 1993), w2segmotion (Lakshmanan *et al*, 2003, 2009; Lakshmanan and Smith, 2009, 2010), time-domain spatial grid objects (TDOs: Davis *et al*, 2006), and various types of upgraded approaches (e.g. ETITAN: Han *et al*, 2009). TDOs, which we employ as the basic metric in this study, are the two- or three-dimensional extent of a contiguous precipitation cluster through time (e.g. Sellars *et al*, 2013). They can be described as an object whose horizontal extent is based on the area of a precipitation cluster at any given time (e.g. derived from single radar scans), and whose vertical extent is based on how long the cluster lasts (e.g. derived from multiple overlaid scans). Recent studies have demonstrated the utility of TDOs in a range of applications and that they can inherently remove some noise in radar data (Clark *et al*, 2012, 2014; Lakshmanan and Kain, 2012; Kain *et al*, 2013; Lakshmanan *et al*, 2013; Burghardt *et al*, 2014).

Another issue facing researchers is the wide range of convective initiation definitions in the literature (Table 1). Many of these definitions are developed and applied by those manually recording convective initiation events. As a result, the rules employed by these studies are geared towards human-researcher capabilities (Wilson and Schreiber, 1986; Wilson and Mueller, 1993; Medlin and Croft, 1998; Dixon and Mote, 2003; Roberts and Rutledge, 2003; Mecikalski and Bedka, 2006; Frye and Mote, 2010; Weckwerth *et al*, 2011). More recent research has implemented objective approaches such as using existing storm-tracking algorithms to detect convective initiation occurrences automatically (Lima and Wilson, 2008; Davini *et al*, 2011; Duda and Gallus, 2013; Kain *et al*, 2013; Burghardt *et al*, 2014; Clark *et al*, 2014; Fabry and Cazenave, 2014; Lock and Houston, 2014). The definitions used for convective initiation in these studies were typically related to how the researchers intended to use the resulting data. For example, Kain *et al* (2013) and Burghardt *et al* (2014) used convective initiation occurrence data to test the spatio-temporal accuracy of numerical model solutions, and Lock and Houston (2014) required events to be separated by 100 km to eliminate double counting of meteorological parameters associated with affected grid cells.

3. Data and methodology

The purpose of this study is to assess the impact of urbanisation on ICI. Although ICI events have not been climatologically characterized around Atlanta, case-studies and model simulations (Dixon and Mote, 2003; Shepherd, 2005) led us to hypothesize that ICI events occurred more often over and near the city. Further, we wanted to ascertain if potential differences between urban and rural ICI counts always exist or if a particular time period is favoured. To simulate the spatial distribution of ICI in the absence of Atlanta, the tests were repeated for a rural control area in proximity to the city. Studies have reported that regions climatologically downwind from an urban area experience more rainfall on average (Rose *et al*, 2008; Hand and Shepherd, 2009); therefore, we also assessed the impact of prevailing winds on ICI distribution.

3.1. Study region description

The study region primarily consists of the northern half of Georgia and extreme northeast Alabama (Figure 1). Elevation in this region is at a minimum of 200 m in west-central Georgia and a maximum of 1471 m in the Appalachian Mountains in extreme northeast Georgia. The natural land cover is dominated by deciduous trees with pockets of evergreen forests that become more widespread in the southern portion of the study area. The region also has widespread agricultural land use, including hay fields and/or pastures. The study region provides stark contrasts

Table 1. A selection of radar-based convective initiation definitions employed in the literature.

Study	Rate threshold	Distance threshold	Temporal threshold	Comments
Wilson and Schreiber (1986)	$\geq$ 30 dBZ	Cannot be attached to existing convection	None	Reflectivity at 1 km above ground level
Wilson and Mueller (1993)	$\geq$ 30 dBZ	Cannot be attached to existing convection	None	–
Medlin and Croft (1998)	$\geq$ 29 dBZ	Must be the first initiation of day	None	No cloud cover or remnant convection could be present
Outlaw and Murphy (2000)	$\geq$ 30 dBZ	231 km	2 h	If dBZ was <30, grid cell must be covered at least 20%
Dixon and Mote (2003)	None	Must not occur when convection is ongoing in area	None	Manual selection
Roberts and Rutledge (2003)	$\geq$ 35 dBZ	None	None	–
Mecikalski and Bedka (2006)	$\geq$ 35 dBZ	None	None	Uses a cloud mask
Lima and Wilson (2008)	> 35 dBZ	None	None	TITAN
Frye and Mote (2010)	$\geq$ 35 dBZ	Must be isolated	None	Manual selection
Davini *et al* (2011)	$\geq$ 40 dBZ	None	None	Storm tracking resembles SCIT
Weckwerth *et al* (2011)	$\geq$ 28 dBZ	Cannot be attached to existing convection	15 min	Manual selection
Duda and Gallus (2013)	$\geq$ 3 mm h^{-1}	None	None	Stage IV first hour $\geq$3 mm was observed
Kain *et al* (2013)	$\geq$ 35 dBZ	40 km	30 min	At -10° C, National Mosaic and Quantitative Precipitation Estimation (NMQ)
Burghardt *et al* (2014)	$\geq$ 35 dBZ	13 km	30 min	At -10° C, National Mosaic and Quantitative Precipitation Estimation (NMQ)
Clark *et al* (2014)	$\geq$ 2.54 and $\geq$6.35 mm h^{-1}	8, 16 and 32 km	30 min	Stage IV
Fabry and Cazenave (2014)	$\geq$ 40 dBZ	30 km	None	No convection within 30 km of new echo in last 30 min
Lock and Houston (2014)	None	100 km	30 min	–

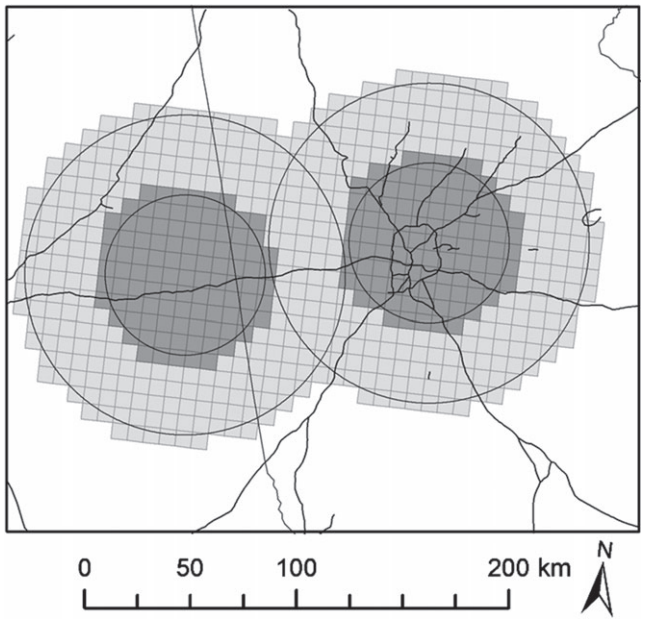

Figure 1. Study area with urban (darker squares) and rural (lighter squares) 8 km grids associated with Atlanta (right) and the control region (left). Overlaid are state boundaries and major regional highways.

between developed land use and natural/agricultural land cover/land use that are ideal for addressing the research question posed by this investigation. The region experiences 340–900 mm of rainfall (PRISM Climate Group, 2004) each year from May to September, with a maximum near the Appalachian Mountains.

3.2. Data

Four datasets were used to explore the effects of urban land use on ICI during the months of May–September from 1997 to 2013: the Spatial Synoptic Classification database, the 2006 National Land Cover Database (NLCD), NOAA archived soundings for KFFC (Peachtree City, WMO 72215), and NOWrad^{TM} composite radar data. Daily spatial synoptic classification (SSC: Sheridan, 2002) data were acquired for the Atlanta, Georgia station (ATL) for May–September for each year in the study period (1997–2013). We only considered a subset of days in this period that were classified as moist tropical (MT), or labelled specifically as 'MT', 'MT+', or 'MT++' by the SSC (Mote *et al*, 2007; Ashley *et al*, 2012; Bentley *et al*, 2012). These types of day experience conditional instability, exhibit a marked urban/rural temperature difference, and have been used by previous studies to control for synoptic forcing (Kalkstein *et al*, 1996; Sheridan *et al*, 2000; Sheridan, 2002; Mote *et al*, 2007; Ashley *et al*, 2012; Bentley *et al*, 2012). We then processed sequences of 5 min NOWrad^{TM} national composite reflectivity data (Parker and Knievel, 2005) with timestamps that correspond to an MT day to extract ICI events in the study region that occurred during synoptically benign conditions (this process is outlined in the next section). A 40 km circular buffer, centred on the centroid of the NLCD-derived boundary of Atlanta, was used to delineate the spatial extent of the developed land use (similar to Ashley *et al*, 2012). This area was bounded by another buffer extending outward an additional 40 km to capture regions of sparsely developed land around the city for purposes of comparing event counts between the two regions. Two equally sized and similarly oriented buffers (i.e. a 40 km buffer within an 80 km buffer) were then placed approximately 150 km west of Atlanta to serve as the rural control region for the study (Figure 1), which is similar to the control method employed by Ashley *et al* (2012). We used the simplified delineation of Atlanta because there were no changes to our results and conclusions when we employed the more intricate approaches such as buffering areas within 5 km of major highways (Dixon and Mote, 2003), or using an NLCD-derived boundary around Atlanta's developed land use (Ashley *et al*, 2012). Finally, to assess the effect of prevailing wind on ICI location relative to the urban area, 700 hPa wind observations at KFFC (approximately 50 km southwest of downtown Atlanta) were associated with each qualifying event.

3.3. Land-use/land-cover induced isolated convective initiation detection algorithm

3.3.1. Algorithm design

Our automated method of detecting urban-induced ICI is, in part, based on the approach presented by Dixon and Mote

(2003). Initially, our goal was to develop a technique that would allow us to feasibly search sequences of radar images for ICI events during 'convectively complicated' situations that were not considered for the analysis completed by Dixon and Mote (2003). To achieve this objective, however, development of a more intricate method of detecting ICI events was necessary to handle complex convective scenarios and other issues associated with automated processing of radar data.

For our period of record, bloom, biological echoes and other sources of noise apparent in radar data can impact long-term aggregations of events (Parker and Knievel, 2005; Lakshmanan *et al*, 2013). Use of a reflectivity threshold can eliminate some erroneous echoes from the data (e.g. 40 dBZ: Parker and Knievel, 2005). To remove further noise in radar images, recent work has employed an object-based approach when accumulating data over a long period. Specifically, TDOs have been illustrated by Lakshmanan *et al* (2013) as an effective method to reduce noise in radar-derived climatologies.

Less obvious forcing mechanisms, such as outflow boundaries emanating from existing cells, can also impact the spatial analysis of ICI. Studies have addressed this issue by disqualifying any convective initiation event if it is within a particular distance of convectively active pixels (Wilson and Schreiber, 1986; Wilson and Mueller, 1993; Frye and Mote, 2010; Weckwerth *et al*, 2011; Kain *et al*, 2013; Burghardt *et al*, 2014; Clark *et al*, 2014; Fabry and Cazenave, 2014; Lock and Houston, 2014). Although some of these studies used qualitative rules to qualify or disqualify convective initiation events (i.e. 'cannot *be attached to*', 'must *be isolated*'), the assessment of large amounts of data makes manual examination rules unfeasible. Instead, recent work has utilized strict exclusion distance thresholds to allow the process to be automated and transparent (Kain *et al*, 2013; Burghardt *et al*, 2014; Clark *et al*, 2014; Fabry and Cazenave, 2014; Lock and Houston, 2014).

To develop an effectual definition of ICI, we first compiled test periods in which different storm modes and evolution were apparent in the radar data. Specifically, days with few isolated cells, merging and splitting cells, mesoscale convective systems, and even tropical system passages were chosen to qualitatively assess the robustness of our procedure. We tested three variables during this analysis: the reflectivity threshold, the exclusion buffer size, and the longevity requirement of the developing cell. Although our desired outcomes were subjective, we assessed the behaviour of each threshold tested by viewing animations with ICI location output locations and compared these to our expected results.

For buffer sizes, we tested exclusion distances from 1 to 120 km. We found that buffer sizes over 30 km excluded too many events, and sizes smaller than this generally included too many 'attached' events or events likely to have been forced by propagating outflow boundaries. Our longevity threshold was tested with values between 0 and 120 min and similarly we found a 30 min threshold was ideal for the purposes of our study. A 30 min threshold has also been employed by recent studies to avoid considering noise or 'failed storms' as a qualifying event (Weckwerth *et al*, 2011; Kain *et al*, 2013; Burghardt *et al*, 2014; Clark *et al*, 2014; Lock and Houston, 2014). For our reflectivity threshold, we tested values between 30 and 50 dBZ and found 40 dBZ to be ideal in reducing artefacts in the accumulated grid maps. This threshold is also an established value for depicting regions of convection in radar images (Davini *et al*, 2011; Ashley *et al*, 2012; Fabry and Cazenave, 2014). In summary, we used TDOs to build the two-dimensional (x,y) evolution of each cell through time, requiring that qualifying events must meet or exceed a 40 dBZ threshold, their location must be greater than 30 km from existing convection, and the initial cluster of convectively active pixels must develop into a storm that lasts at least 30 min.

3.3.2. Procedure

The TDO algorithm was run on a set of radar images with timestamps that occurred on Atlanta MT days between May and September from 1997 to 2013. We defined the MT day as starting at 1200 UTC on the SSC date to 1159 UTC on the day after the SSC date. For example, if 2 May 2012 was classified as an MT day, we gathered all available radar images between 1200 UTC on 2 May 2012 and 1159 UTC on 3 May 2012. This was done to include the entire diurnal 'convective cycle' in the analysis. The algorithm operated on a moving window of a set of eight images. This was sufficient to determine areas of existing convection, locations of new, independent convection and to follow the development of convection for half an hour.

Our ICI detection process (Figure 2) was run on eight temporally contiguous images at a time. The first image (a) in the eight-scan run is used to identify existing convectively active ($\geq$40 dBZ) pixels (b), and around these pixels a 30 km buffer is created (c). Convectively active pixels from the second image (d) are identified (e), and if any of these pixels are within the 30 km buffer (f), they are removed (g). Convectively active pixels for the next six images are identified (h) and are 'stacked' sequentially (i). The isolated, new, convectively active pixels layer from the second image (g) is inserted at the bottom of the stack and three-dimensional, 26 connected neighbourhoods clustering on the seven-scan stack (j) is performed. Finally, for every qualifying TDO (k), the centroid of the oldest (e.g. the bottom layer) two-dimensional convectively active cluster is calculated and the date, time, latitude, longitude and 700 hPa wind associated with that ICI event are stored and used for conducting spatial analyses. We see many other clusters can exist (l) but most were associated with ongoing convective clusters or those that initiated after the second image (d).

4. Results

4.1. Overview

Overall, 25 995 ICI events were detected in the study area between May and September for the 17-year period (Figure 3). On average, the study area experiences 1530 ICI events per year on MT days, with a minimum of 759 events in 1999 and a maximum of 3037 in 2010. The study region averages 28 ICI events per MT day (henceforth, ICI day^{-1}), with a minimum of 19.0 ICI day^{-1} in 1999 and a maximum of 36.2 ICI day^{-1} in 2006 (Figure 4). These results are comparable in magnitude to other reported findings for similarly sized study areas: namely Frye and Mote (2010) and Davini *et al* (2011) who recorded approximately 9 ICI day^{-1} and 16 ICI day^{-1}, respectively. The most prolific ICI-producing day in the study area coincided with the disastrous northern Georgia flooding described in Shepherd *et al* (2011) when 109 ICI events occurred between 1200 UTC on 20 September 2009 and 1200 UTC on 21 September 2009. Nearly record-breaking precipitable water values, moderate convective available potential energy, and favourable low- and mid-level winds supportive of training and redevelopment of convective cells were in place during this case (Shepherd *et al*, 2011).

June and July are the most active months of the warm season with a mean of 15.6 and 14.7 ICI day^{-1}, respectively. Similarly, existing lightning and thunderstorm climatologies have illustrated convective activity maximizes in July in the southeast United States (Hodanish *et al*, 1997; Geerts, 1998; Changnon, 2001; Dixon and Mote, 2003; Hill *et al*, 2010). Further, visual inspection of ICI event density maps suggest that, relative to the study area, the strongest urban signal occurs in July (Figure 5). Diurnally, ICI event counts begin to increase between 1500 and 1700 UTC and reach a maximum during the 2000 UTC hour (Figure 6). After 2000 UTC, the study region experiences a sharp decrease in ICI events until a minimum is reached at 1400 UTC. During the warm season, some parts of the United States, including the Southeast and Colorado Front Range, experience a 'peaked' diurnal cycle of convection in which thunderstorm activity sharply increases during the late morning, maximizes in the afternoon, and decreases overnight (Carbone and Tuttle, 2008). In the

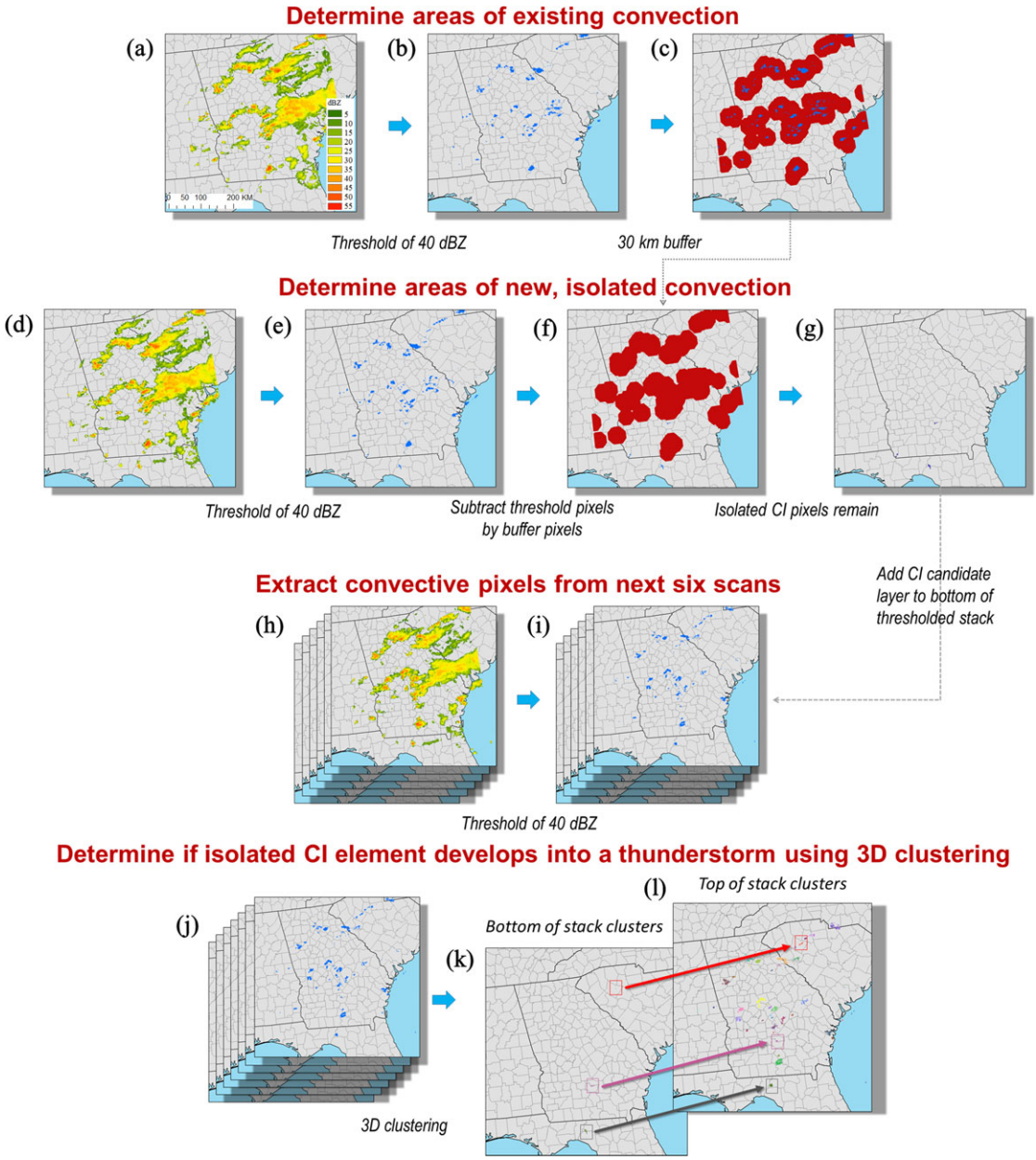

Figure 2. (a)–(l) Schematic of the process used in this study to detect isolated, persisting, convective initiation events.

Southeast, this is thought to be due to the local (mesoscale) nature of convective forcing and the sensitivity of convective development to diurnal heating during the warm-season months (Carbone and Tuttle, 2008). Our results show that ICI occurrence is also tied to this 'peaked' pattern in convective activity and analogous temporal ICI analyses have presented similar results (Davini *et al*, 2011; Weckwerth *et al*, 2011).

For the 40 km inner buffer delineating Atlanta, ICI day^{-1} ranged from less than 1 in 1999 to 2.7 in 2003. On average, Atlanta experiences 1.8 ICI day^{-1}, in contrast to 1.7 ICI day^{-1} for the control area (Figure 4). At 2.2 ICI day^{-1}, July is the most active month for Atlanta with a seasonal maximum in CI point density over the urban area (Figure 5). Although the ICI day^{-1} counts are comparable between the two regions, Atlanta experiences a markedly different diurnal cycle compared to the control region (Figure 6). The divergence occurs when the late morning increase in ICI events for Atlanta begins to level out between 1700 and 1900 UTC. In contrast, ICI counts for the control region increase steadily until 2000 UTC. Thereafter, ICI occurrences for Atlanta increase after 2000 UTC and remain steady until 2300 UTC while the control region experiences decreasing ICI occurrences after 2000 UTC. Specifically, Atlanta experienced 126% more ICI events than the control region between 2000 and 0100 UTC for the period of record.

4.2. *ICI count comparisons between regions*

We first generated 2, 4, 6, 8 and 16 km grids for the study area to determine the various distributions of ICI counts per grid cell. For smaller grid cell sizes, there were numerous cells with counts of zeros or ones which produced an exponential distribution. As grid cell size increased, a log-normal distribution of ICI counts became apparent. We ultimately chose 8 km grid cells as a compromise between fine resolution and a near-normal distribution of ICI counts per cell. However, due to the non-normal distribution of the counts, a non-parametric statistical test (i.e. Mann–Whitney U: Mann and Whitney, 1947) was employed with an alpha value of 0.05. For each comparison, we report the U-statistic (U) and the p-value (p). One caveat of using the Mann-Whitney U test for this study is that the grid cell values may not be independent and, as a result, the reported p-values may be lower than what they should be. We employed two approaches to minimize dependence: (i) only consider the ICI event centroid when generating the climatology, and (ii) ICI events could not occur within 30 km of another event at the same time. However, these considerations do not completely eliminate the issue of grid cell dependence. Thus, further comparisons are made between these results, visual analyses, and Local Indicators of Spatial Association (LISA: Anselin, 1995) analysis maps because

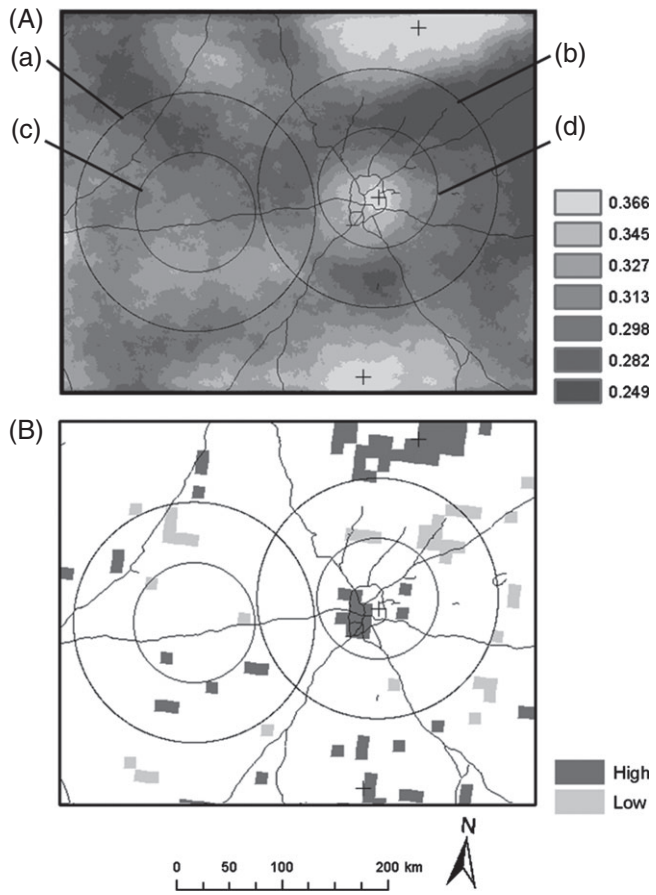

Figure 3. (A) 1 km ICI point density in 30 km neighbourhoods for the study area during the period of record (moist tropical days, May–September, 1997–2013). Buffer (a) and (b) represent the 80 km buffers centred on the control region and Atlanta (respectively) and buffer (c) and (d) are the 40 km 'urban' buffers for the control and Atlanta (respectively). The '+' denotes the centroids of three areas with the highest regional ICI point density. These areas are, from north to south: the Appalachian Mountains, the northeast loop of Atlanta, and the Pine Mountain in central Georgia. (B) LISA analysis showing significant high ICI count clustering (darker squares) and significant low ICI count clustering (lighter squares) per 8 km grid cell.

of the spatial autocorrelation that may exist in samples of spatially gridded values. LISA measures local spatial autocorrelation and is useful for determining the significance of local spatial clustering of high and low values in a regional context.

Overall, mean ICI count per grid cell was significantly ($U = 7337$, $p < 0.001$) higher for the 8 km urban grids (mean: 21.7) compared to the rural grids (mean: 18.7) for the buffers centred on Atlanta. In comparison, the control region west of the city experienced a mean ICI count per grid cell of 19.8 for the urban and rural surrogate buffers. June (urban: 3.6, rural: 3.1), July (urban: 6.6, rural: 5.6), and August (urban: 6.3, rural: 5.3) all produced significantly ($U_{\text{june}} = 9393$, $p_{\text{june}} = 0.04$; $U_{\text{july}} = 8684$, $p_{\text{july}} = 0.004$; $U_{\text{august}} = 8473$, $p_{\text{august}} = 0.002$) higher mean ICI count per grid cell ICI event density over Atlanta than the surrounding rural region. ICI event density maps and LISA analysis also suggest that a significant local maximum exists within the inner 40 km buffer centred on Atlanta overall and, specifically, during the months of June, July and August. These results prompted further statistical and visual investigation of the spatio-temporal nature of ICI events for the two regions.

4.2.1. *Hourly analysis*

To assess what times of the day, if any, produced significant urban/rural differences, ICI counts per grid cell were calculated for eight 3 h subsets (i.e. 1200–1500, 1500–1800 UTC, and so on). Using the buffers in Figure 1, comparisons were made between counts per 8 km urban and rural grid cells to determine what time periods produce significantly more ICI events over the city compared to the surrounding rural land. Both periods between 2100 and 0300 UTC produced significantly ($U_{2100-0000} = 5731$, $p_{2100-0000} < 0.001$; $U_{0000-0300} = 8697$, $p_{0000-0300} = 0.004$) more ICI events within the urban grids for the Atlanta buffer. Although the overall urban/rural difference is stronger than for this specific period, the contributions from each subset other than the two periods between 2100 and 0300 UTC are not significant on their own. For the control region, there was no significant difference between the urban and rural ICI counts for the overall period of record or any 3 h period (Figure 7).

A visual inspection of study area ICI development between 1200 and 2100 UTC revealed a relationship between higher ICI occurrence and areas of higher elevation. Specifically, the southern portions of the Blue Ridge Mountains and the Cumberland Plateau in northern Georgia and northeastern Alabama, respectively, as well as the Pine Ridge Mountain in west-central Georgia are associated with regional maxima in ICI event density (Figure 7(a–c)). Similar results were found during the Convective and Orographically-induced Precipitation Study (Wulfmeyer *et al,* 2011) – –particularly, convective initiation was found to occur earlier in the day over areas with higher elevation compared to those with lower elevation (Weckwerth *et al,* 2011). A marked increase in ICI occurrence then takes place over northern Atlanta between 2100 and 0000 UTC (d), which then shifts to the southern and eastern portions of the city by 0000–0300 UTC (e). This regional maximum over the city largely dissipates after 0300 UTC (f–h), at which time areas

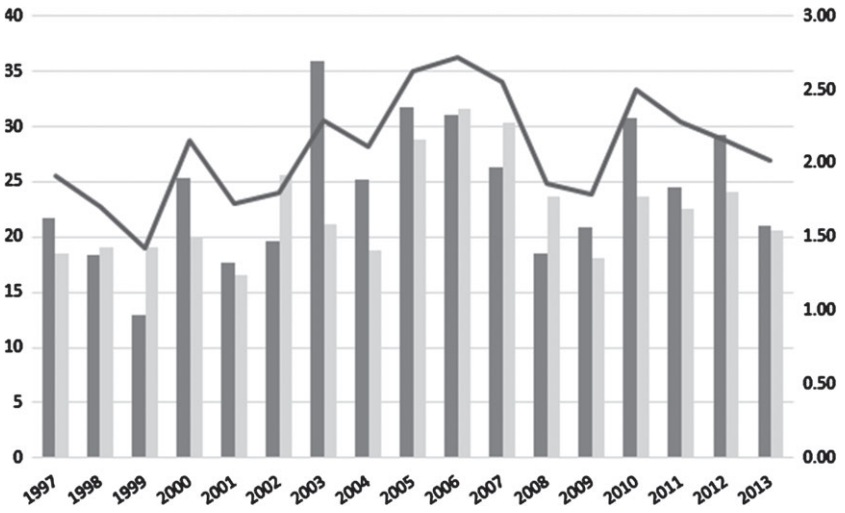

Figure 4. Yearly ICI counts per moist tropical day for the study region (dark line, left *y*-axis), the 40 km Atlanta buffer (darker bars, right *y*-axis) and control buffer (lighter bars, right *y*-axis).

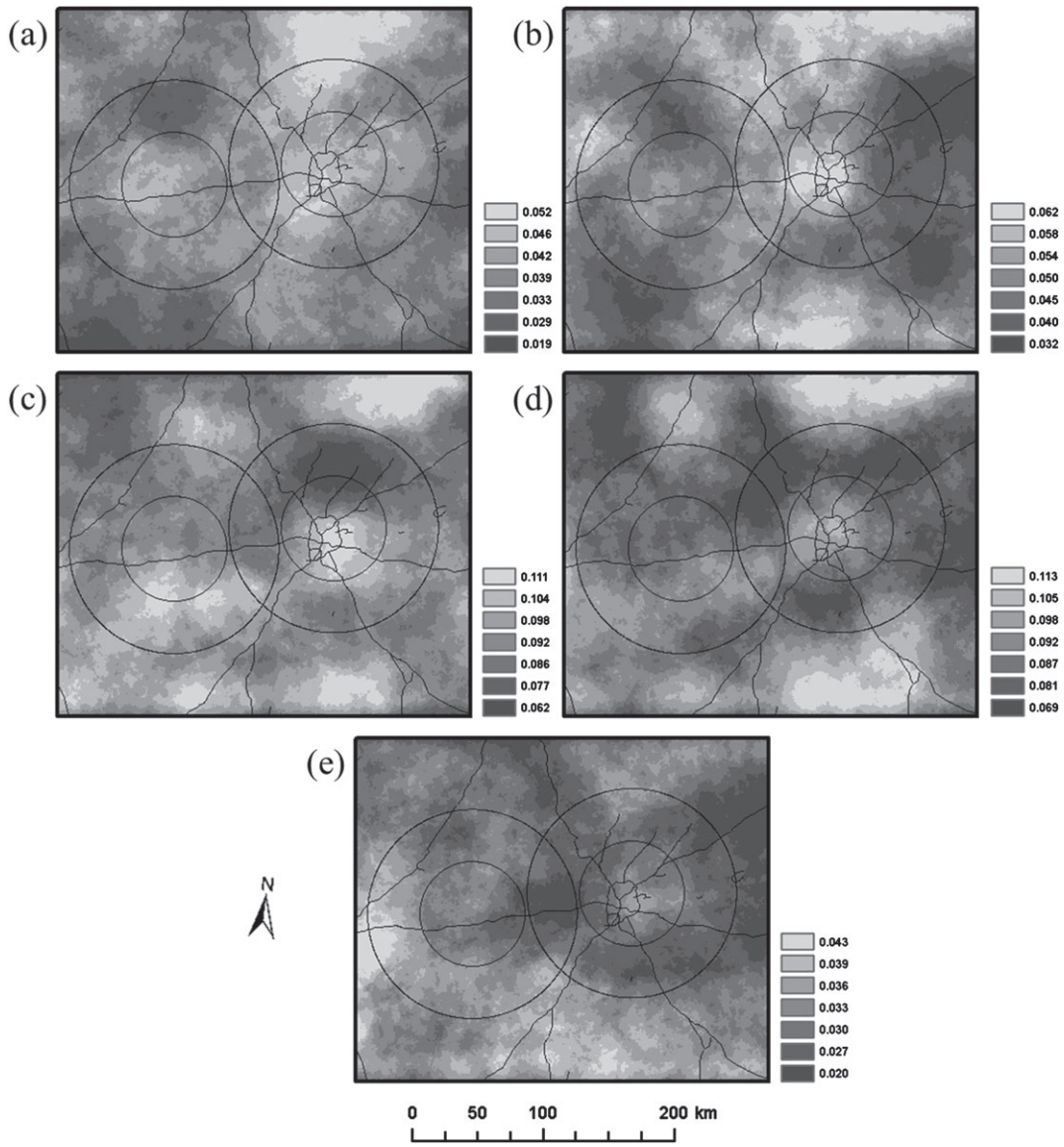

Figure 5. 1 km ICI density for 30 km neighbourhoods during moist tropical days for each month (1997–2013), (a) May to (e) September, respectively.

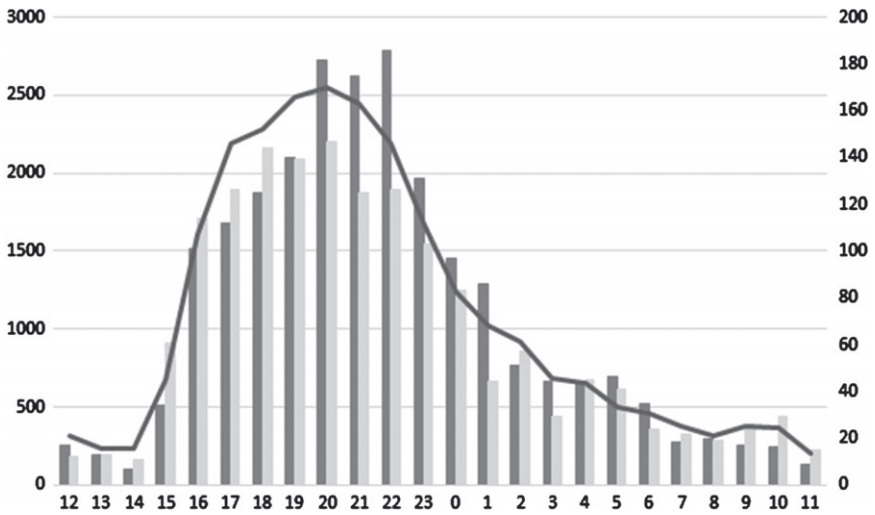

Figure 6. The count of ICI events during moist tropical days per hour (UTC) for the study region (dark line, left *y*-axis), the 40 km Atlanta buffer (darker bars, right *y*-axis) and control buffer (lighter bars, right *y*-axis).

of higher elevation again experience regional maxima in ICI occurrence. These results suggest that developed land use induces convection primarily during a 6 h period in the late afternoon and early evening during synoptically benign days. However, since Atlanta is situated in a region with complex terrain, the potential effects of mountain/valley circulations on the ICI climatology cannot be ignored. For example, Svoma (2010) reported that the nocturnal maximum in convective activity over an urban area near complex terrain (i.e. Phoenix, AZ) could be influenced by high and low elevation interactions that are independent of any urban contributions to convective enhancement. Since ICI activity peaks over areas of higher terrain earlier in the day (b,c),

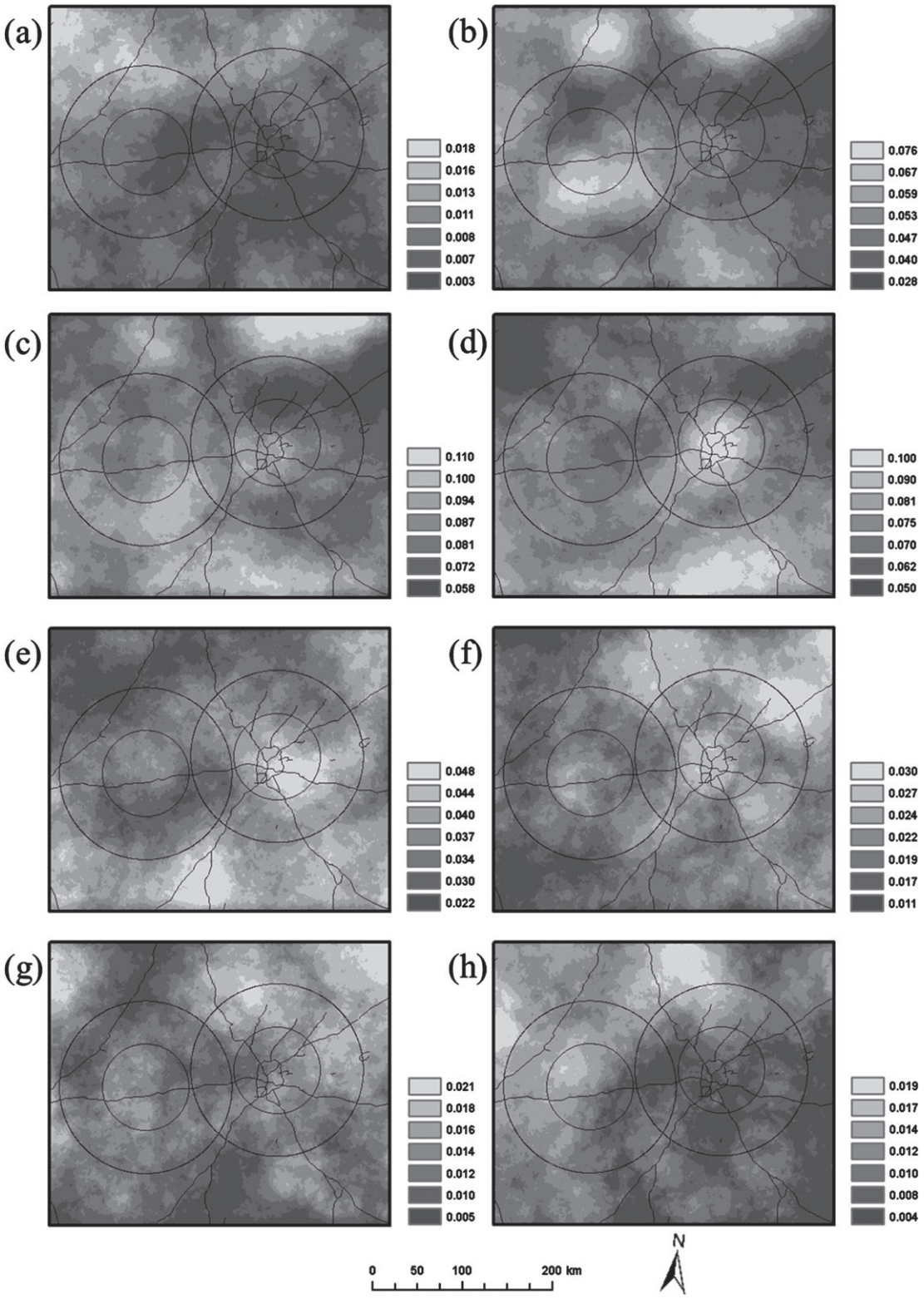

Figure 7. 1 km ICI density for 30 km neighbourhoods during moist tropical days, May–September (1997–2013), between the hours of (a) 1200–1500 UTC, (b) 1500–1800 UTC, (c) 1800–2100 UTC, (d) 2100–0000 UTC, (e) 0000–0300 UTC, (f) 0300–0600 UTC, (g) 0600–0900 UTC, and (h) 0900–1200 UTC.

it is possible that convective activity over these regions may have an effect on the timing and placement of ICI events later in the day. In the following sections, we present evidence that day of the week and prevailing wind direction also have an influence on the spatial distribution of ICI occurrence, but only around the city and not the control region. These results support the hypothesis that urbanisation associated with Atlanta is a dominant forcing mechanism for convective activity in the region.

Although our results differ from the only previous work on CI around Atlanta (i.e. Dixon and Mote, 2003), Shepherd (2004) has suggested that the procedure employed by that study to detect urban initiated thunderstorm events may be too restrictive by disqualifying cases due to ongoing regional convection, especially during the afternoon. Our study approached the issue of convective contamination by assuring new cells were relatively isolated on an objective case-by-case basis, which permitted more daytime ICI events to be included. As a result, the timing of the maximum urban effect on ICI occurrences more closely resembles the timing of maximum thunderstorm occurrence reported in existing regional radar climatologies (e.g. Mote *et al*, 2007; Parker and Ahijevych, 2007; Carbone and Tuttle, 2008). The late afternoon might represent an optimal combination of instability and differential heating as the rural areas surrounding Atlanta cool. Future observational and modelling studies may be needed

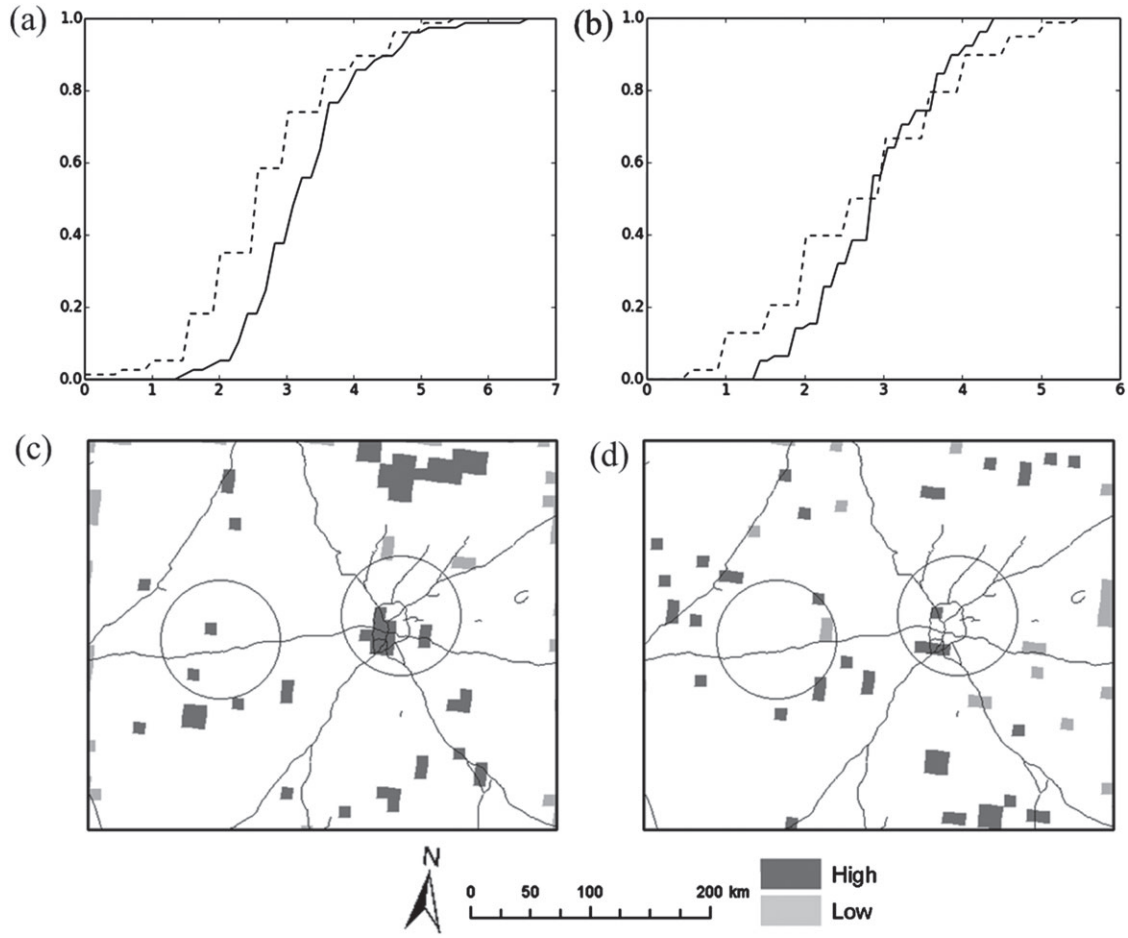

Figure 8. (a,b) Cumulative probability density plots for normalized moist tropical weekend (dotted) and weekday (solid) ICI counts per 8 km grid for (a) Atlanta and (b) the control. (c,d) LISA spatial autocorrelation analysis maps for (c) weekdays and (d) weekends using an inverse squared distance search approach. Darker (lighter) squares represent significant high (low) value clustering relative to the overall study area counts per 8 km grid cell.

to explore combinations of ingredients related to forcing ICI over Atlanta.

4.2.2. *Weekend/weekday analysis*

Ambient aerosol levels have been measured in higher quantities during the week compared to the weekend in and near highly developed areas (Tao *et al,* 2012). Existing studies have used this to their advantage when designing methods to test the impacts of urban aerosols on precipitation. Specifically, precipitation rates on weekdays have been compared to weekends to explore this relationship (e.g. Cerveny and Balling, 1998; Bell *et al*, 2008; Svoma and Balling, 2009; Tuttle and Carbone, 2011; Stallins *et al*, 2013). To assess the potential impact of urban-related aerosols on ICI over and near Atlanta, we compared ICI counts on the weekends and weekdays for urban grid cells in the Atlanta and the control buffers. We defined weekday ICI events as events that occurred between 1200 UTC on Monday morning and 1159 UTC on Saturday morning, whereas all other events were considered weekend events. Weekday (weekend) ICI events were aggregated to 8 km grids and normalized by dividing ICI counts per grid by 5 (2).

There was no significant ($U = 2779$, $p = 0.17$) difference between weekend and weekday counts for the control (Figure 8). In contrast, Atlanta had significantly ($U = 1905$, $p < 0.001$) more ICI events on weekdays than at the weekend (a,b), with the highest mean ICI count per 8 km grid occurring on Tuesday (mean: 3.6) and Wednesday (mean: 3.2) and the lowest occurring on Saturday (mean: 2.8) and Sunday (mean: 2.4). Tuesday and Wednesday alone had significantly ($U = 1833$, $p < 0.001$) greater ICI counts per grid cell than did the rest of the week. The LISA results also support these findings with more grid cells exhibiting significant high-value clustering within the 40 km inner buffer centred on Atlanta on weekdays compared to weekends (c,d).

Although large-scale studies of the southeast United States have found evidence of a midweek increase in precipitation thought to be caused by anthropogenic aerosols (Bell *et al*, 2008; Tuttle and Carbone, 2011; Stallins *et al*, 2013), modelling studies have concluded that ICI occurrence should not be modified by higher or lower ambient aerosol levels (van den Heever and Cotton, 2007). Despite the fact warm-rain processes are thought to be delayed or inhibited by an increased amount of cloud condensation nuclei (CCN: Tao *et al*, 2012), longevity, updraught strength and electrification can all be enhanced by higher ambient aerosol levels (van den Heever and Cotton, 2007; Tao *et al*, 2012). Further, when storms reach the intensity required by this study (i.e. 40 dBZ), they may have existed as a vertically developed cloud for a half an hour or more (Roberts and Rutledge, 2003; Lock and Houston, 2014). Thus, it is possible that eventual thunderstorms develop on the upwind edges of Atlanta's urban land use and then begin to interact with increasing levels of aerosols as they move downwind of the city. Ultimately, this would allow for storms to last longer and produce taller and stronger updraughts, which would make aerosol-modified storms more likely to be associated with ICI as defined in our study. Our results suggest that although the effects of convergence and instability provided by the UHI and increased surface roughness are important in initiating storms, aerosols emanating from the city can encourage ICI in events where the incipient storm might have otherwise dissipated. Although this indicates that higher ambient aerosol levels increase the likelihood of ICI, our understanding of this relationship is still weak (Tuttle and Carbone, 2011), and disagreement still exists in the literature (e.g. Rosenfeld, 2000; Kaufmann *et al*, 2007; van den Heever and Cotton, 2007; Bell *et al*, 2008; Koren *et al*, 2008; Lacke *et al*, 2009; Coquillat *et al*, 2012; Diem, 2013; Stallins *et al*, 2013).

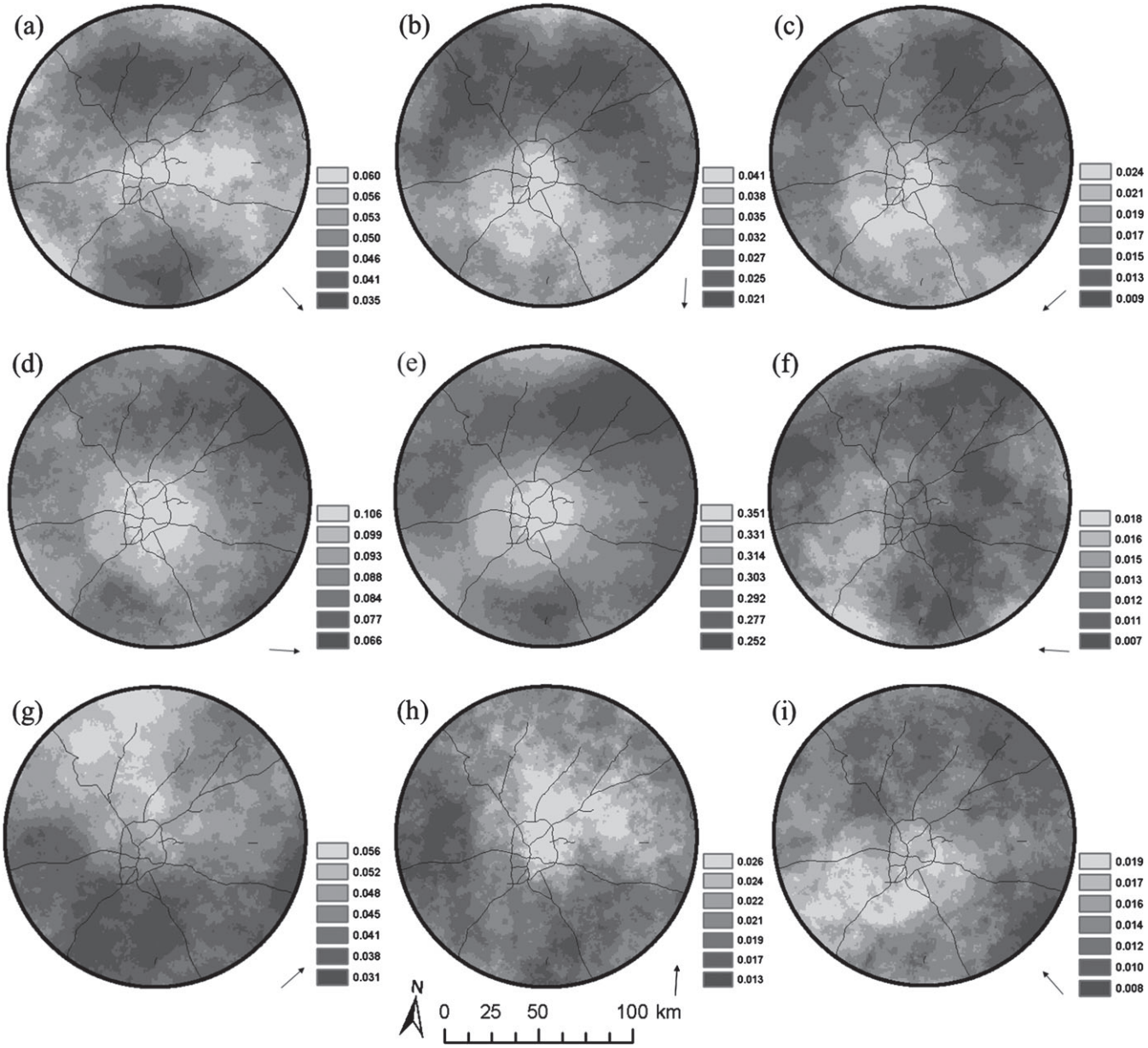

Figure 9. 1 km ICI density in a 30 km neighbourhood (moist tropical days, May–September, 1997–2013) in the 80 km Atlanta buffer during moist tropical days when 700 hPa winds were from the (a) northwest, (b) north, (c) northeast, (d) west, (e) overall, (f) east, (g) southwest, (h) south, and (i) southeast. The arrows represent the direction of winds at 700 hPa for each circle.

4.2.3. Steering wind analysis

We then examined the impact of particular wind regimes on the spatial distribution of ICI counts per grid cell. To do this, the 80 km Atlanta and control region buffers were divided into two halves along a line perpendicular to eight different steering wind directions (i.e. 700 hPa: Rose *et al*, 2008; Hand and Shepherd, 2009; Ganeshan *et al*, 2013), and 8 km grids with ICI counts during days with particular 700 hPa wind directions were separated into upwind and downwind groups. Rather than using the climatological mean wind direction, this approach allowed us to approximate the probable movement of storms in the area on an event-by-event basis (Rose *et al* 2008; Niyogi *et al*, 2011). Mean wind speed at 700 hPa during ICI events was approximately 7.7 m s^{-1} and did not differ greatly between the wind directions we tested.

Overall, there were significantly ($U = 713\,888$, $p < 0.001$) more ICI occurrences per grid cell for downwind regions compared to upwind regions in the Atlanta buffer. Statistical tests also revealed that there were significantly higher ICI counts in downwind regions, relative to Atlanta, during days with north ($U = 8814$, $p < 0.001$), northeast ($U = 10\,256$, $p = 0.008$), northwest ($U = 10\,421$, $p = 0.016$) and southwest winds ($U = 10\,478$, $p = 0.019$) at 700 hPa. A visual inspection of the ICI point density analysis for the Atlanta buffer supports these statistical findings (Figure 9). In particular, a noticeable visual signal was evident on all three of the wind directions with a northerly component (a,b,c), with a weaker relationship for south and southwest winds (g,h). West winds (d) produced a point density maximum slightly east of the overall maximum, and east and southeast winds produced maxima seemingly unrelated to wind direction. In contrast, no noticeable signal was evident in the point density analysis for the control buffer.

Although this is the first climatological depiction of the effect of prevailing wind direction on the location of ICI relative to a large urban area, numerical approaches have presented evidence that locations downwind of a large city should be favoured regions for thunderstorm initiation (Baik *et al*, 2001, 2007; Han *et al*, 2012). Observationally, Niyogi *et al* (2011) found that downwind areas relative to Indianapolis experienced significantly smaller thunderstorm cell size (a climatological proxy for favoured convective initiation locations) than upwind areas. These findings also contribute to the understanding of studies that have noted a downwind maximum in radar-derived rainfall totals and lightning occurrence relative to the urban area (Shepherd *et al*, 2002; Burian and Shepherd, 2005; Rose *et al*, 2008; Hand and Shepherd, 2009)

and naturally occurring boundaries such as those associated with spatial discontinuities in soil moisture and vegetation (Taylor *et al*, 2007, 2010; Garcia-Carreras *et al*, 2010; Garcia-Carreras and Parker, 2011). Namely, we provide evidence that the development of new cells, along with urban enhancement and bifurcation of existing cells (e.g. Bornstein and Lin, 2000) contribute to the downwind convective precipitation maximum relative to urban areas.

5. Conclusions

Parker and Knievel (2005) noted that as the size of radar data repositories increase with time, even subtle patterns in these data could be revealed as significant. Since then, a number of studies have employed radar data to examine billions of samples of high-resolution instantaneous rainfall rates and uncover previously unobserved rainfall patterns. A subset of these works have used these data to explore the link between developed land use and convective activity (e.g. Mote *et al*, 2007; Bentley *et al*, 2010, 2012; Ashley *et al*, 2012; Stallins *et al*, 2012). This study extends those endeavours and reveals the relationship between independent, convective initiation events and developed land-use morphologies.

A specific algorithm was developed to detect ICI, a phenomenon that is difficult to quantitatively define. Through exploratory analysis and a detailed survey of the existing literature, the procedure was developed, tested and utilized in one of the first objective climatological analyses of ICI events. The output from this algorithm was then used to explore the spatio-temporal nature of ICI in and around Atlanta, as well as a nearby rural control. The strongest signal revealed by this study was the late afternoon maximum in ICI occurrences over and downwind of Atlanta. The most obvious implication of this finding is that commuters in and around Atlanta may be exposed to sudden-onset thunderstorm hazards during the evening rush hour. Quickly deteriorating conditions associated with independent ICI could catch drivers unaware as roadways could become slick or flooded quickly, as was the case in September 2009 (Shepherd *et al*, 2011). The time of maximum ICI occurrences for Atlanta also coincides with after-work and after-school activities – many of which take place outside. This leads to an enhanced risk of exposure to sudden thunderstorm hazards, such as strong winds or lightning (Stallins, 2002), for vulnerable populations that may have limited or no quick access to shelter. Residents and meteorologists in Atlanta and other similar urban environments could use the results presented to increase awareness of the nature of hazards associated with thunderstorms (Stallins, 2004; Stewart *et al*, 2004).

Finally, a weekday/weekend dichotomy in ICI occurrences was revealed for Atlanta – namely that the city and adjacent regions experienced significantly higher normalized ICI counts during the week compared to the weekend. Although the existing literature related to aerosol effects on precipitation report diverse results (Tuttle and Carbone, 2011; Tao *et al*, 2012), the findings of this study could help direct future observational and modelling studies. Specifically, a more in-depth, and possibly day-by-day, analysis with observations of ambient levels of various-sized aerosols could be performed to uncover more specific relationships between aerosols and ICI. Future studies could also look at the impact of higher and lower reflectivity thresholds (e.g. 30, 50 dBZ) to see if more intense storms are occurring during weekdays compared to the weekend over Atlanta.

Acknowledgements

The authors would like to thank Phil Young (Director, NIU Department of Geography's Geovisual Mapping Laboratory) and Arthur Person (Senior Research Assistant at The Pennsylvania State University, Department of Meteorology) for allowing us to use their computing resources. We would also like to thank Andrew Krmenec and David Changnon for their helpful suggestions. Further, we would like to thank two anonymous reviewers and Douglas Parker for their suggested revisions and additions.

References

Altaratz O, Ilan K, Yoav Y, Price C. 2010. Lightning response to smoke from Amazonian fires. *Geophys. Res. Lett.* **37**: L07801, doi: 10.1029/2010GL042679.

Anselin L. 1995. Local indicators of spatial association: LISA. *Geogr. Anal.* **27**: 93–115, doi: 10.1111/j.1538-4632.1995.tb00338.x.

Ashley WS, Bentley ML, Stallins JA. 2012. Urban-induced thunderstorm modification in the southeast United States. *Clim. Change* **113**: 481–498, doi: 10.1007/s10584-011-0324-1.

Ashley WS, Strader S, Rosencrants T, Krmenec AJ. 2014. Spatiotemporal changes in tornado hazard exposure: The case of the expanding bull's eye effect in Chicago, IL. *Weather Clim. Soc.* **6**: 175–193, doi: 10.1175/WCAS-D-13-00047.1.

Baik J, Kim Y, Chun H. 2001. Dry and moist convection forced by an urban heat island. *J. Appl. Meteorol.* **40**: 1462–1475, doi: 10.1175/1520-0450(2001)040<1462:DAMCFB>2.0.CO;2.

Baik JJ, Kim YH, Kim JJ, Han JY. 2007. Effects of boundary-layer stability on urban heat island-induced circulation. *Theor. Appl. Climatol.* **89**: 73–81.

Bell TL, Rosenfeld D, Kim K-M, Yoo J-M, Lee M-I, Hahnenberger M. 2008. Midweek increase in US summer rain and storm heights suggests air pollution invigorates rainstorms. *J. Geophys. Res.* **113**: D02209, doi: 10.1029/2007JD008623.

Bentley ML, Stallins JA. 2005. Climatology of cloud to ground lightning in Georgia, USA, 1992–2003. *Int. J. Climatol.* **25**: 1979–1996, doi: 10.1002/joc.1227.

Bentley ML, Stallins JA, Ashley WS. 2010. The Atlanta thunderstorm effect. *Weatherwise* **63**: 24–29, doi: 10.1080/00431671003609937.

Bentley ML, Stallins JA, Ashley WS. 2012. Synoptic environments favourable for urban convection in Atlanta, Georgia. *Int. J. Climatol.* **32**: 1287–1294, doi: 10.1002/joc.2344.

Blumenfeld KA. 2008. *Convective Weather Hazards in the Twin Cities Metropolitan Area, MN*. ProQuest LLC: Ann Arbor, MI.

Bornstein R, Lin Q. 2000. Urban heat islands and summertime convective thunderstorms in Atlanta: Three case studies. *Atmos. Environ.* **34**: 507–516.

Burghardt BJ, Evans C, Roebber PJ. 2014. Assessing the predictability of convection initiation in the high plains using an object-based approach. *Weather and Forecasting* **29**: 403–418, doi: 10.1175/WAF-D-13-00089.1.

Burian SJ, Shepherd JM. 2005. Effect of urbanization on the diurnal rainfall pattern in Houston. *Hydrol. Process.* **19**: 1089–1103, doi: 10.1002/hyp.5647.

Carbone RE, Tuttle JD. 2008. Rainfall occurrence in the US warm season: The diurnal cycle. *J. Clim.* **21**: 4132–4146, doi: 10.1175/2008JCLI2275.1.

Cerveny RS, Balling RC. 1998. Weekly cycles of air pollutants, precipitation and tropical cyclones in the coastal NW Atlantic region. *Nature* **394**: 561–563.

Changnon SA. 2001. Thunderstorm rainfall in the conterminous United States. *Bull. Am. Meteorol. Soc.* **82**: 1925–1940.

Clark AJ, Kain JS, Marsh PT, Correia J Jr, Xue M, Kong F. 2012. Forecasting tornado pathlengths using a three-dimensional object identification algorithm applied to convection-allowing forecasts. *Weather and Forecasting* **27**: 1090–1113.

Clark AJ, Bullock RG, Jensen TL, Xue M, Kong F. 2014. Application of object-based time-domain diagnostics for tracking precipitation systems in convection-allowing models. *Weather and Forecasting* **29**: 517–542, doi: 10.1175/WAF-D-13-00098.1.

Coquillat S, Boussaton M, Buguet M, Lambert D, Ribaud J, Berthelot A. 2012. Lightning ground flash patterns over Paris area between 1992 and 2003: Influence of pollution? *Atmos. Res.* **122**: 77–92, doi: 10.1016/j.atmosres.2012.10.032.

Davini P, Bechini R, Cremonini R, Cassardo C. 2011. Radar-based analysis of convective storms over northwestern Italy. *Atmosphere* **3**: 33–58, doi: 10.3390/atmos3010033.

Davis C, Brown B, Bullock R. 2006. Object-based verification of precipitation forecasts. Part I: Methodology and application to mesoscale rain areas. *Mon. Weather Rev.* **134**: 1772–1784, doi: 10.1175/MWR3145.1.

Diem JE. 2013. The 1970 Clean Air Act and termination of rainfall suppression in a US urban area. *Atmos. Environ.* **75**: 141–146, doi: 10.1016/j.atmosenv.2013.04.041.

Dixon PG, Mote TL. 2003. Patterns and causes of Atlanta's urban heat island-initiated precipitation. *J. Appl. Meteorol.* **42**: 1273–1284, doi: 10.1175/1520-0450(2003)042<1273:PACOAU>2.0.CO;2.

Dixon M, Wiener G. 1993. TITAN: Thunderstorm identification, tracking, analysis, and nowcasting – a radar-based methodology. *J. Atmos. Oceanic Technol.* **10**: 785–797, doi: 10.1175/1520-0426(1993)010<0785:TTITAA>2.0.CO;2.

Duda JD, Gallus WA. 2013. The impact of large-scale forcing on skill of simulated convective initiation and upscale evolution with convection-allowing grid spacings in the WRF. *Weather and Forecasting* **28**: 994–1018, doi: 10.1175/WAF-D-13-00005.1.

Fabry F, Cazenave Q. 2014. From severe weather climatologies to the impact of cities, or what we can learn from 17 years of US radar composites. In

94th National AMS Meeting, Paper 2.4. American Meterological Society: Atlanta, GA.

Frye JD, Mote TL. 2010. Convection initiation along soil moisture boundaries in the southern Great Plains. *Mon. Weather Rev.* **138**: 1140–1151, doi: 10.1175/2009MWR2865.1.

Ganeshan M, Murtugudde R, Imhoff ML. 2013. A multi-city analysis of the UHI-influence on warm season rainfall. *Urban Clim.* **6**: 1–23, doi: 10.1016/j.uclim.2013.09.004.

Garcia-Carreras L, Parker DJ. 2011. How does local tropical deforestation affect rainfall? *Geophys. Res. Lett.* **38**: L19802, doi: 10.1029/2011GL049099.

Garcia-Carreras L, Parker DJ, Taylor CM, Reeves CE, Murphy JG. 2010. Impact of mesoscale vegetation heterogeneities on the dynamical and thermodynamic properties of the planetary boundary layer. *J. Geophys. Res.* **115**: D03102, doi: 10.1029/2009JD012811.

Gauthier ML, Petersen WA, Carey LD. 2010. Cell mergers and their impact on cloud-to-ground lightning over the Houston area. *Atmos. Res.* **96**: 626–632, doi: 10.1016/j.atmosres.2010.02.010.

Geerts B. 1998. Mesoscale convective systems in the southeast United States during 1994–1995: A survey. *Weather and Forecasting* **13**: 860–869, doi: 10.1175/1520-0434(1998)013<0860:MCSITS>2.0.CO;2.

Georgescu M, Morefield PE, Bierwagen BG, Weaver CP. 2014. Urban adaptation can roll back warming of emerging megapolitan regions. *Proc. Natl. Acad. Sci. U.S.A.* **111**: 2909–2914.

Han L, Fu S, Zhao L, Zheng Y, Wang H, Lin Y. 2009. 3D convective storm identification, tracking, and forecasting – an enhanced TITAN algorithm. *J. Atmos. Oceanic Technol.* **26**: 719–732, doi: 10.1175/2008JTECHA1084.1.

Han J, Baik J, Khain AP. 2012. A numerical study of urban aerosol impacts on clouds and precipitation. *J. Atmos. Sci.* **69**: 504–520.

Hand LM, Shepherd JM. 2009. An investigation of warm-season spatial rainfall variability in Oklahoma City: Possible linkages to urbanization and prevailing wind. *J. Appl. Meteorol. Climatol.* **48**: 251–269, doi: 10.1175/2008JAMC2036.1.

van den Heever SC, Cotton WR. 2007. Urban aerosol impacts on downwind convective storms. *J. Appl. Meteorol. Clim.* **46**: 828–850, doi: 10.1175/JAM2492.1.

Hill CM, Fitzpatrick PJ, Corbin JH, Lau YH, Bhate SK. 2010. Summertime precipitation regimes associated with the sea breeze and land breeze in southern Mississippi and eastern Louisiana. *Weather and Forecasting* **25**: 1755–1779, doi: 10.1175/2010WAF2222340.1.

Hodanish S, Sharp D, Collins W, Paxton C, Orville RE. 1997. A 10-yr monthly lightning climatology of Florida: 1986–1995. *Weather and Forecasting* **12**: 439–448.

Huff FA, Changnon SA. 1973. Precipitation modification by major urban areas. *Bull. Am. Meteorol. Soc.* **54**: 1220–1232, doi: 10.1175/1520-0477(1973)054<1220:PMBMUA>2.0.CO;2.

Johnson JT, MacKeen PL, Witt A, Mitchell EDW, Stumpf GJ, Eilts MD, Thomas KW. 1998. The storm cell identification and tracking algorithm: An enhanced WSR-88D algorithm. *Weather and Forecasting* **12**: 263–276, doi: 10.1175/1520-0434(1998)013<0263:TSCIAT>2.0.CO;2.

Kain JS, Coniglio MC, Correia J Jr, Clark AJ, Marsh PT, Ziegler CL, Lakshmanan V, Miller SD Jr, Dembek SR, Weiss SJ, Kong F, Xue M, Sobash RA, Dean AR, Jirak IL, Melick CJ. 2013. A feasibility study for probabilistic convection initiation forecasts based on explicit numerical guidance. *Bull. Am. Meteorol. Soc.* **94**: 1213–1225, doi: 10.1175/BAMS-D-11-00264.1.

Kalkstein LS, Nichols MC, Barthel CD, Greene JS. 1996. A new spatial synoptic classification: Application to air mass analysis. *Int. J. Climatol.* **16**: 983–1004, doi: 10.1002/(SICI)1097-0088(199609)16:9<983::AID-JOC61>3.0.CO;2-N.

Kaufmann RK, Seto KC, Schneider A, Liu Z, Zhou L, Wang W. 2007. Climate response to rapid urban growth: Evidence of a human-induced precipitation deficit. *J. Clim.* **20**: 2299–2306, doi: 10.1175/JCLI4109.1.

Koren I, Martins JV, Remer LA, Afargan H. 2008. Smoke invigoration versus inhibition of clouds over the Amazon. *Science* **321**: 946–949, doi: 10.1126/science.1159185.

Lacke MC, Mote TL, Shepherd JM. 2009. Aerosols and associated precipitation patterns in Atlanta. *Atmos. Environ.* **43**: 4359–4373.

Lakshmanan V, Kain JS. 2012. 'Detecting convective initiation using radar images'. In *Proceedings, 7th European Conference on Radar in Meteorology and Hydrology, ERAD*, Toulouse, France, 25–29 June 2012, 198 pp.

Lakshmanan V, Smith T. 2009. Data mining storm attributes from spatial grids. *J. Atmos. Oceanic Technol.* **26**: 2353–2365.

Lakshmanan V, Smith T. 2010. An objective method of evaluating and devising storm-tracking algorithms. *Weather and Forecasting* **25**: 701–709, doi: 10.1175/2009WAF2222330.1.

Lakshmanan V, Rabin R, DeBrunner V. 2003. Multiscale storm identification and forecast. *Atmos. Res.* **67**: 367–380.

Lakshmanan V, Hondl K, Rabin R. 2009. An efficient, general-purpose technique for identifying storm cells in geospatial images. *J. Atmos. Oceanic Technol.* **26**: 523–537, doi: 10.1175/2008JTECHA1153.1.

Lakshmanan V, Miller M, Smith T. 2013. Quality control of accumulated fields by applying spatial and temporal constraints. *J. Atmos. Oceanic Technol.* **30**: 745–758, doi: 10.1175/JTECH-D-12-00128.1.

Lang TJ, Rutledge SA. 2011. A framework for the statistical analysis of large radar and lightning datasets: Results from STEPS 2000. *Mon. Weather Rev.* **139**: 2536–2551, doi: 10.1175/MWR-D-10-05000.1.

Lima MA, Wilson JW. 2008. Convective storm initiation in a moist tropical environment. *Mon. Weather Rev.* **136**: 1847–1864, doi: 10.1175/2007MWR2279.1.

Lock NA, Houston AL. 2014. Empirical examination of the factors regulating thunderstorm initiation. *Mon. Weather Rev.* **142**: 240–258, doi: 10.1175/MWR-D-13-00082.1.

Lowry WP. 1998. Urban effects on precipitation amount. *Prog. Phys. Geog.* **22**: 477–520, doi: 10.1177/030913339802200403.

Mahmood R, Pielke RA Sr, Hubbard KG, Niyogi D, Bonan G, Lawrence P, McNider R, McAlpine C, Etter A, Gameda S, Qian BD, Carleton A, Beltran-Przekurat A, Chase T, Quintanar AI, Adegoke JO, Vezhapparambu S, Conner G, Asefi S, Sertel E, Legates DR, Wu YL, Hale R, Frauenfeld ON, Watts A, Shepherd M, Mitra C, Anantharaj VG, Fall S, Lund R, Nordfelt A, Blanken P, Du JY, Chang H-I, Leeper R, Nair US, Dobler S, Deo R, Syktus J. 2010. Impacts of land use/land cover change on climate and future research priorities. *Bull. Am. Meteorol. Soc.* **91**: 37–46.

Mahmood R, Pielke RA, Hubbard KG, Niyogi D, Dirmeyer PA, McAlpine C, Carleton AM, Hale R, Gameda S, Beltran-Przekurat A, Baker B, McNider R, Legates DR, Shepherd JM, Du J, Blanken PD, Fraudenfeld OW, Nair US, Fall S. 2014. Land cover changes and their biogeophysical effects on climate. *Int. J. Climatol.* **34**: 929–953.

Mann HB, Whitney DR. 1947. On a test of whether one of two random variables is stochastically larger than the other. *Ann. Math. Stat.* **18**: 50–60.

Matyas CJ. 2010. Use of ground-based radar for climate-scale studies of weather and rainfall. *Geogr. Compass* **4**: 1218–1237.

Mecikalski JR, Bedka KM. 2006. Forecasting convective initiation by monitoring the evolution of moving cumulus in daytime GOES imagery. *Mon. Weather Rev.* **134**: 49–78, doi: 10.1175/MWR3062.1.

Medlin JM, Croft PJ. 1998. A preliminary investigation and diagnosis of weak shear summertime convective initiation for extreme southwest Alabama. *Weather and Forecasting* **13**: 717–728, doi: 10.1175/1520-0434(1998)013<0717:APIADO>2.0.CO;2.

Mote TL, Lacke MC, Shepherd JM. 2007. Radar signatures of the urban effect on precipitation distribution: A case study for Atlanta, Georgia. *Geophys. Res. Lett.* **34**: L20710, doi: 10.1029/2007GL031903.

Niyogi D, Pyle P, Lei M, Arya SP, Kishtawal CM, Shepherd JM, Chen F, Wolfe B. 2011. Urban modification of thunderstorms: An observational storm climatology and model case study for the Indianapolis urban region. *J. Appl. Meteorol. Clim.* **50**: 1129–1144, doi: 10.1175/2010JAMC1836.1.

Nowak DJ, Walton JT. 2005. Projected urban growth (2000–2050) and its estimated impact on the US forest resource. *J. Forest.* **103**: 383–389.

Oke TR. 1973. City size and the urban heat island. *Atmos. Environ.* **7**: 769–779, doi: 10.1016/0004-6981.

Outlaw DE, Murphy MP. 2000. *A Radar-Based Climatology of July Convective Initiation in Georgia and Surrounding Area,* NOAA Eastern Region Technical Attachment No. 2000-04. US National Weather Service: Greenville-Spartanburg, SC.

Parker MD, Ahijevych DA. 2007. Convective episodes in the east-central United States. *Mon. Weather Rev.* **135**: 3707–3727, doi: 10.1175/2007MWR2098.1.

Parker MD, Knievel JC. 2005. Do meteorologists suppress thunderstorms?: Radar-derived statistics and the behavior of moist convection. *Bull. Am. Meteorol. Soc.* **86**: 341–358, doi: 10.1175/BAMS-86-3-341.

Paulikas MJ, Ashley WS. 2011. Thunderstorm hazard vulnerability for the Atlanta, Georgia metropolitan region. *Nat. Hazards* **58**: 1077–1092, doi: 10.1007/s11069-010-9712-5.

PRISM Climate Group. 2004. Oregon State University. http://prism.oregonstate.edu (accessed 1 November 2014).

Rinehart RE, Garvey ET. 1978. Three-dimensional storm motion detection by conventional weather radar. *Nature* **273**: 287–289, doi: 10.1038/273287a0.

Roberts RD, Rutledge S. 2003. Nowcasting storm initiation and growth using GOES-8 and WSR-88D data. *Weather and Forecasting* **18**: 562–584, doi: 10.1175/1520-0434(2003)018<0562:NSIAGU>2.0.CO;2.

Rose LS, Stallins JA, Bentley ML. 2008. Concurrent cloud-to-ground lightning and precipitation enhancement in the Atlanta, Georgia (United States), urban region. *Earth Interact.* **12**: 1–30, doi: 10.1175/2008EI265.1.

Rosenfeld D. 2000. Suppression of rain and snow by urban and industrial air pollution. *Science* **287**: 1793–1796, doi: 10.1126/science.287.5459.1793.

Sellars S, Nguyen P, Chu W, Gao XG, Hsu K-L, Sorooshian S. 2013. Computational Earth science: Big data transformed into insight. *EOS Trans. Am. Geophys. Union* **94**: 277–278, doi: 10.1002/2013EO320001.

Shepherd JM. 2004. Comments on Rainfall modification by major urban areas: Observations from spaceborne rain radar on the TRMM satellite – reply. *J. Appl. Meteorol.* **43**: 951–957.

Shepherd JM. 2005. A review of current investigations of urban-induced rainfall and recommendations for the future. *Earth Interact.* **9**: 1–27, doi: 10.1175/EI156.1.

Shepherd JM, Burian SJ. 2003. Detection of urban-induced rainfall anomalies in a major coastal city. *Earth Interact.* **7**: 1–17.

Shepherd JM, Pierce H, Negri AJ. 2002. Rainfall modification by major urban areas: Observations from spaceborne rain radar on the TRMM satellite. *J. Appl. Meteorol.* **41**: 689–701, doi: 10.1175/1520-0450(2002)041<0689:RMBMUA>2.0.CO;2.

Shepherd JM, Mote T, Dowd J, Roden M, Knox P, McCutcheon SC, Nelson SE. 2011. An overview of synoptic and mesoscale factors contributing to the disastrous Atlanta flood of 2009. *Bull. Am. Meteorol. Soc.* **92**: 861–870, doi: 10.1175/2010BAMS3003.1.

Sheridan SC. 2002. The redevelopment of a weather-type classification scheme for North America. *Int. J. Climatol.* **22**: 51–68, doi: 10.1002/joc.709.

Sheridan SC, Kalkstein LS, Scott JM. 2000. An evaluation of the variability of air mass character between urban and rural areas. In *Biometeorology and Urban Climatology at the Turn of the Millennium*: 487–490. World Meteorological Organization: Geneva, Switzerland.

Stallins JA. 2002. An overlooked source of weather-related property damage in the Southeast: Lightning losses for Georgia, 1996–2000. *Southeast. Geogr.* **42**: 296–301, doi: 10.1353/sgo.2002.0026.

Stallins JA. 2004. Characteristics of urban lightning hazards for Atlanta, Georgia. *Clim. Change* **66**: 137–150.

Stallins JA, Bentley ML, Rose LS. 2005. Cloud-to-ground flash patterns for Atlanta, Georgia (USA) from 1992 to 2003. *Clim. Res.* **30**: 99–112.

Stallins JA, Carpenter J, Bentley ML, Ashley WS, Mulholland JA. 2013. Weekend–weekday aerosols and geographic variability in cloud-to-ground lightning for the urban region of Atlanta, Georgia, USA. *Reg. Environ. Change* **13**: 137–151, doi: 10.1007/s10113-012-0327-0.

Stewart TR, Pielke R Jr, Nath R. 2004. Understanding user decision making and the value of improved precipitation forecasts: Lessons from a case study. *Bull. Am. Meteorol. Soc.* **85**: 223–235, doi: 10.1175/BAMS-85-2-223.

Svoma BM. 2010. The influence of monsoonal gulf surges on precipitation and diurnal precipitation patterns in central Arizona. *Weather and Forecasting* **25**: 281–289.

Svoma BM, Balling RC Jr. 2009. An anthropogenic signal in Phoenix Arizona winter precipitation. *Theor. Appl. Climatol.* **98**: 315–321.

Tao W-K, Chen J-P, Li ZQ, Wang C, Zhang CD. 2012. Impact of aerosols on convective clouds and precipitation. *Rev. Geophys.* **50**: RG2001, doi: 10.1029/2011RG000369.

Taylor CM, Parker DJ, Harris PP. 2007. An observational case study of mesoscale atmospheric circulations induced by soil moisture. *Geophys. Res. Lett.* **34**: L15801, doi: 10.1029/2007GL030572.

Taylor CM, Harris PP, Parker DJ. 2010. Impact of soil moisture on the development of a Sahelian mesoscale convective system: A case-study from the AMMA Special Observing Period. *Q. J. R. Meteorol. Soc.* **136**: 456–470, doi: 10.1002/qj.465.

Theobald DM. 2005. Landscape patterns of exurban growth in the USA from 1980 to 2020. *Ecol. Soc.* **10**: 32.

Tuttle JD, Carbone RE. 2011. Inferences of weekly cycles in summertime rainfall. *J. Geophys. Res.* **116**: D20213, doi: 10.1029/2011JD 015819.

Weckwerth TM, Wilson JW, Hagen M, Emerson TJ, Pinto JO, Rife DL, Grebe L. 2011. Radar climatology of the COPS region. *Q. J. R. Meteorol. Soc.* **146**: 31–41, doi: 10.1002/qj.747.

Wilson JW, Mueller CK. 1993. Nowcasts of thunderstorm initiation and evolution. *Weather and Forecasting* **8**: 113–131, doi: 10.1175/1520-0493(1986)114<2516:IOCSAR>2.0.CO;2.

Wilson JW, Schreiber JW. 1986. Initiation of convective storms at radar-observed boundary-layer convergence lines. *Mon. Weather Rev.* **114**: 2516–2536, doi: 10.1175/1520-0493(1986)114<2516:IOCSAR>2.0.CO;2.

Wulfmeyer V, Behrendt A, Kottmeier C, Corsmeier U, Barthlott C, Craig GC, Hagen M, Althausen D, Aoshima F, Arpagaus M, Bauer H, Bennett L, Blyth A, Brandau C, Champollion C, Crewel S, Dick G, Girolamo PD, Dorninger M, Dufournet Y, Eigenmann R, Engelmann R, Flamant C, Foken T, Gorgas T, Grzeschik M, Handwerker J, Hauck C, Holler H, Junkermann W, Kalthoff N, Kiemle C, Klink S, Konig M, Krauss L, Long CH, Madonna F, Mobbs SD, Neininger B, Pal S, Peters G, Pigeon G, Richard E, Rotach MW, Russchenberg H, Schwitalla T, Smith V, Steinacker R, Trentmann J, Turner DD, van Baelen J, Vogt S, Volkert H, Weckwerth TM, Wernli H, Wieser A, Wirth M. 2011. The Convective and Orographically-induced Precipitation Study (COPS): The scientific strategy, the field phase, and research highlights. *Q. J. R. Meteorol. Soc.* **137**: 3–30.

